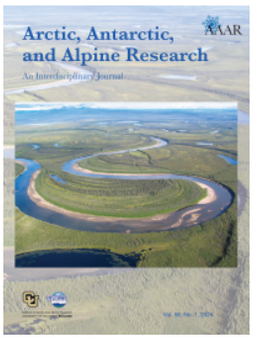

Taylor & Francis
Taylor & Francis Group

Arctic, Antarctic, and Alpine Research

An Interdisciplinary Journal

ISSN: (Print) (Online) Journal homepage: www.tandfonline.com/journals/uaar20

Distribution and composition of redox-active species and dissolved organic carbon in Arctic lacustrine porewaters

Danhui Xin, Jeffrey M. Hudson, Anthony Sigman-Lowery & Yu-Ping Chin

To cite this article: Danhui Xin, Jeffrey M. Hudson, Anthony Sigman-Lowery & Yu-Ping Chin (2024) Distribution and composition of redox-active species and dissolved organic carbon in Arctic lacustrine porewaters, Arctic, Antarctic, and Alpine Research, 56:1, 2371534, DOI: 10.1080/15230430.2024.2371534

To link to this article: https://doi.org/10.1080/15230430.2024.2371534

ARCTIC, ANTARCTIC, AND ALPINE RESEARCH
2024, VOL. 56, NO. 1, 2371534
https://doi.org/10.1080/15230430.2024.2371534

Taylor & Francis
Taylor & Francis Group

Distribution and composition of redox-active species and dissolved organic carbon in Arctic lacustrine porewaters

Danhui Xin[a,b], Jeffrey M. Hudson[c], Anthony Sigman-Lowery[a], and Yu-Ping Chin[a]

[a]Department of Civil and Environmental Engineering, University of Delaware, Newark, Delaware, USA; [b]Southern California Coastal Water Research Project Authority, Costa Mesa, California, USA; [c]OHSU/PSU School of Public Health, Oregon Health & Science University, Portland, Oregon, USA

ABSTRACT

The interaction between redox-active species and dissolved organic carbon (DOC) is crucial in driving lacustrine benthic microbial processes. In lacustrine porewaters, many redox-active species exist in their reduced form, while DOC acts as a substrate and an electron acceptor. Understanding the types and abundance of redox-active species in porewaters along with their complementary DOC substrate is pivotal for gaining insights into benthic processes, particularly in regions susceptible to climate change. We report the *in-situ* measurement of redox-active species in sediment porewaters, alongside the *ex-situ* measurement of DOC extracted from cores collected from two Arctic lakes (Toolik and Fog 1). Fe^{2+} was abundantly detected below 4 cm of the sediment-water interface in all cores and was inversely related to dissolved O_2. Additionally, two distinct Fe(III)-complexes were identified. DOC ranged in the order of 10s of mg/L and either remained stable or increased with depth. A comparison between Toolik and Fog 1 lakes revealed a higher accumulation of Fe^{2+} and DOC in the latter. This study marks the first of its kind to assess spatial distributions of redox-active species and DOC as a function of depth from multiple sites in Arctic lacustrine porewaters.

ARTICLE HISTORY
Received 29 January 2024
Revised 2 June 2024
Accepted 19 June 2024

KEYWORDS
Arctic; porewater; dissolved organic carbon (DOC); iron; microelectrode

Introduction

Benthic processes, specifically the intricate interplay between redox-active species and dissolved organic carbon (DOC) within lacustrine environments, exert a significant influence on global carbon cycling (Burdige et al. 1992; Thomsen et al. 2004; Dalcin Martins et al. 2017; Trusiak et al. 2018; Barker et al. 2023; Liang et al. 2023). These interactions are multifaceted in nature and pivotal for understanding carbon dynamics. For example, iron oxide minerals can act as terminal electron acceptors (TEAs) to support anaerobic respiration, and the extent to which this occurs is contingent upon the free energies of organic carbon mineralization reactions in sediments (Aeppli et al. 2019, 2022). While the utilization of different TEAs typically follows the "redox ladder" model (Berner 1980; Luther 2016), recent studies have reported robust methanogenesis in the presence of sulfate and even oxygen, challenging existing paradigms and suggesting the need for further investigation on DOC–TEA interactions (Angle et al. 2017; Dalcin Martins et al. 2017). Conversely, iron oxide minerals can encapsulate dissolved organic matter (DOM) at mineral-pore water interfaces via coprecipitation, shielding carbon from microbial respiration (Berner 1980; Kaiser and Guggenberger 2000; Lalonde et al. 2012).

Recent research has documented an increase and a more dynamic pattern in organic carbon inputs in Arctic lakes and wetlands due to permafrost thaw (Walter Anthony et al. 2016), underscoring the urgency of understanding benthic processes in Arctic lakes. Because thawing permafrost constitutes up to 33 percent (1,035 Pg) of the global organic carbon pool (Schuur et al. 2022), identifying the other biogeochemical drivers behind carbon cycling in Arctic lacustrine environments is imperative for a comprehensive understanding of global carbon dynamics.

Assessing the type, distribution, and interaction of two key drivers of benthic processes, i.e., redox-active species and DOC, is the foundational step toward

CONTACT Yu-Ping Chin yochin@udel.edu Department of Civil and Environmental Engineering, University of Delaware, Newark, DE 19716, USA.
Supplemental data for this article can be accessed online at https://doi.org/10.1080/15230430.2024.2371534

understanding the fate of carbon in Arctic lacustrine ecosystems. Many redox-active species present in Arctic lacustrine porewaters (e.g., Fe^{2+} and Mn^{2+}) are reduced products of TEAs (i.e., iron and manganese oxides), formed through microbial respiration. Further, the presence of DOC in porewaters may influence the composition of benthic microbiomes and microbial activity, as it serves as both an electron donor and acceptor (Aeschbacher, Sander, and Schwarzenbach 2010; Wenk et al. 2013; Walpen et al. 2018). Given the perceived patchy distribution of TEAs and the escalating influx of organic carbon into Arctic lacustrine systems from surrounding thermokarsts, profiling the distribution of TEAs and DOC is critical for unraveling the intricate interplay among benthic redox processes, microbiome composition, and, ultimately, carbon cycling.

Voltammetric microelectrodes (Luther et al. 2008; Ma et al. 2008; McAdams et al. 2016; Chan, Emerson, and Luther 2016; Hudson, Michaud, et al. 2022) provide a sophisticated way to profile the vertical distribution of redox-active species associated with TEAs in porewaters with minimal disturbance to the surrounding matrices. Electrodes are amenable to on-site measurements in the field and can quantify multiple peak signals associated with redox-active species at distinct potentials in one scan. When calibrated to concentration, voltammetric electrode data can complement other measurements to develop a holistic view of native redox-active species in porewaters (Druschel et al. 2008; Krepski et al. 2013; Chan, Emerson, and Luther 2016; Hudson et al. 2022). Hudson et al. (2022) deployed voltammetric microelectrodes on multiple sediment cores collected from Toolik Lake (an Alaskan Arctic lake) and coupled the identity and concentrations of redox-active species with 16s rRNA analysis of the benthic microbiome.

To understand the relationship between TEAs and DOM, the distribution of redox-active species and DOC in sedimentary porewaters was quantified for three cores collected from two Alaskan Arctic lakes. We profiled multiple redox-active species, including O_2, Fe^{2+}, Mn^{2+}, and Fe(III)-organic complexes as a function of sediment depth using microelectrodes coupled with cyclic voltammetry (CV). We subsequently extracted the porewaters from the cores for complementary DOC analysis. The addition of DOC data, comparison between two lakes receiving different carbon inputs, and temporal variance between past and current studies yielded insights into the cycling of carbon spatially and temporally in Arctic lacustrine systems.

Materials and methods

Field collection of sediment cores

Sediment cores were collected in July 2022 from two North Slope lakes (Toolik Lake and Fog 1 Lake, Figure 1a) in the Alaskan Arctic. These lakes are located near Toolik Field Station (TFS, 68° 38' N, 149° 36' W), a research facility operated by the University of Alaska

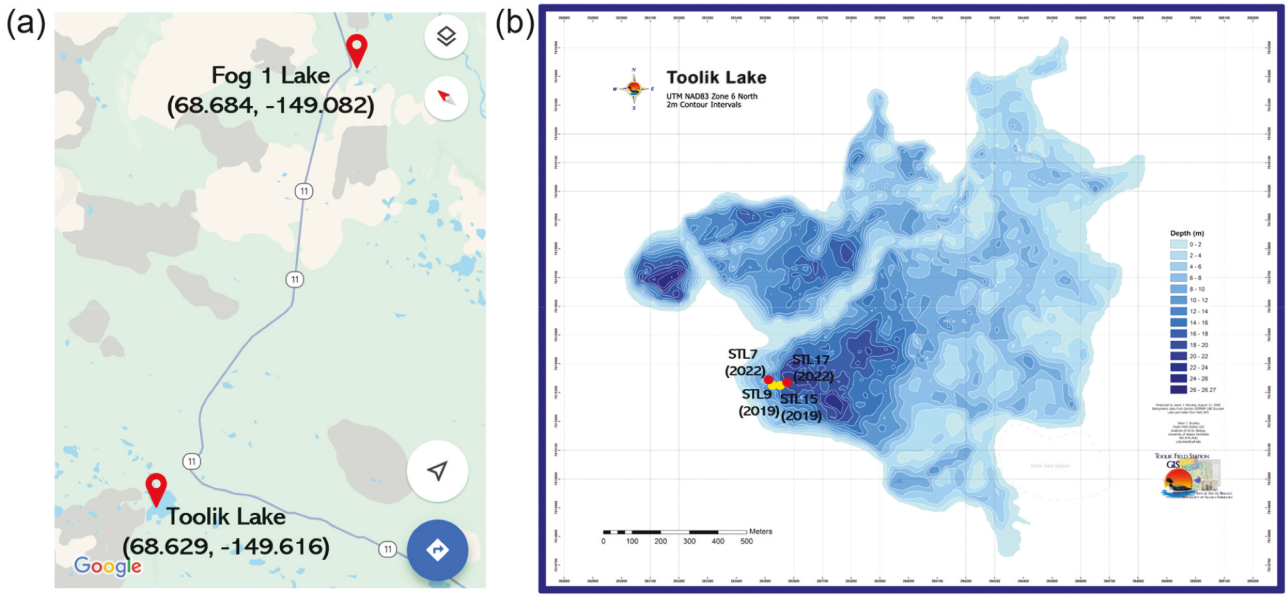

Figure 1. (a) Google Maps image showing the locations (longitude, latitude) of Toolik Lake and Fog 1 Lake. (2) Bathymetry map of Toolik Lake and sampling locations. Red dots represent locations where sediment cores were collected in the year 2022 in this study, whereas yellow dots represent locations of cores collected in 2019 by Hudson et al. (2022).

Fairbanks (UAF) in collaboration with the National Science Foundation (NSF).

Toolik Lake has been continuously monitored and investigated as part of the Arctic Long-Term Ecological Research (LTER) network and more recently as part of the National Ecological Observatory Network (NEON). Toolik Lake is oligotrophic, and rates of organic carbon cycling are slow (Levine and Whalen 2001). Sediment cores from two locations (Figure 1b), one from a shallow site (7 m, STL7) and another from a deeper site (17 m, STL17), were collected on the southwest side of Toolik Lake. Our two cores were collected from adjacent locations where Hudson et al. (2022) collected shallow (9 m, STL9) and deeper (15 m, STL15) cores, respectively, in 2019 for comparison. An additional core (FL) was collected from the middle of Fog 1 Lake, which sits on a watershed that empties into Sagavanirktok River and unlike Toolik Lake, is isolated with no hydrologic inlet or outlet connection to the watershed. The two lakes also differ markedly in their geological ages, lake productivity, and water chemistry (Giblin and Kling 2016).

Coring was conducted using an HTH gravity corer (Pylonex AB, Umeå, Sweden) with a polycarbonate core liner. Sediment cores collected were secured in a milk crate using bungee cords and immediately taken back to TFS for on-site voltammetric analyses and porewater extraction. All cores were analyzed for voltammetry and extracted for porewater within 24 h and 48 h of collection, respectively.

Voltammetric analysis

Before voltammetric analysis, sediment cores were partially extruded to leave at least 5 cm of overlying water above the sediments (Figure S1a) (McAdams et al. 2016). This enabled us to preserve the redox state of sediments below the sediment-water interface (SWI) while allowing us to access the SWI and below with microelectrodes.

CV scans were performed using a portable and wireless potentiostat (STAT-I 400s, Metrohm DropSense, Fountain Valley, CA) controlled by DropView software and a three-electrode system. The three-electrode system consists of a saturated Ag/AgCl reference electrode, a platinum-wire counter electrode, and an Au/Hg amalgam working electrode. Reference and counter electrodes were purchased from BASi (West Lafayette, IN) and used as received. Working electrodes were housed in polyether-ether-ketone (PEEK) tubing and were fabricated and polished in our laboratory at the University of Delaware before the field campaign, following the procedures described in previous marine and sedimentary porewater studies (Luther et al. 2008; McAdams et al. 2016; Hudson et al. 2022). While PEEK electrodes have lower sensitivity than capillary glass electrodes, we have used them successfully in the past as they are more robust and likely to survive the challenges of remote fieldwork (McAdams et al. 2016, 2021; Hudson et al. 2022).

To initiate measurements, reference and counter electrodes were held at the top of the core liner and placed into the overlying water above the SWI. The working electrode was then fastened securely to a millimeter (Narishige, Amityville, NY) allowing vertical adjustment at mm depth resolution, as illustrated in Figure S1b (Supporting Information). The micromanipulator was kept stationary during repeated measurements by locking it to a ring stand using a clamp.

Measurements of redox-active species in the cores were started at 3.5 cm above the SWI and worked down the core at 1 cm intervals until the SWI was reached. Higher resolution measurements at millimeter resolution were applied just below the SWI where the greatest change in redox speciation occurred (Hudson et al. 2022). Cathodic CV scans were performed at scan rates of 1 V/s from −0.1 V to −1.8 V to −0.1 V (vs. Ag/AgCl). CV scans were repeated at each discrete depth at least 3 times until there was no distinct change in the scan, and the final scan was analyzed for redox-active species. Conditioning steps, in which the potential was poised at −0.9 V for 5 s (Shufen et al. 2008), were applied between scans starting at 4 cm below the SWI to remove any previously deposited redox-active species. The CV measurements were repeated twice from the top of the overlying water up to 11 cm below the SWI, and the average and the range of two measurements used (Figure 2).

Prior to measurements, the Au/Hg amalgam working electrode was calibrated for O_2, Fe^{2+}, and Mn^{2+} in each core's respective unfiltered lake water (Toolik Lake water for STL7 and STL17 and Fog 1 Lake water for FL), as detailed in the Supporting Information. Peaks for O_2, Fe^{2+}, and Mn^{2+} occur around respective potentials of −0.32 V, −1.4 V, and −1.55 V (vs. Ag/AgCl). In addition to quantitative analyses of peaks for O_2, Fe^{2+}, or Mn^{2+}, qualitative analyses were conducted for other peaks identified in voltammograms and reported as current (nA). Two distinct peaks were found in between −0.5 V to −0.8 V (vs. Ag/AgCl) in all three cores. Given the abundance of Fe in the Toolik and Fog 1 cores, these peaks are presumably Fe(III)-organic complexes, which are known to reside in the potential range of −0.2 V to −0.9 V (vs. Ag/AgCl) depending on the specific

structure and functional groups of the ligands (Luther et al. 2008; Shufen et al. 2008; Hakala et al. 2009).

Dissolved organic carbon and total metal analysis

After voltammetric analysis was completed, porewaters at discrete depths of sediment cores were withdrawn through pre-drilled ports using a 0.2-µm Rhizon sampler (Rhizosphere Research Products, Wageningen, Netherlands) connected to a 10 mL glass syringe. The porewater was pulled through the Rhizon by applying a vacuum using the syringe. The first 0.5 mL of porewater was discarded after rinsing the Rhizon and syringe. Depending on the availability of porewater, 4–7 mL of porewater samples were collected at 2–4 cm intervals along the depth. Porewater collected in each syringe was transferred to a 15-mL centrifuge tube containing 0.1 mL of 6 N HCl (trace metal grade) and kept on ice at 4°C for shipment from Alaska to our laboratory. Acidification was necessary for sample preservation, the prevention of Fe(II) oxidation (which would influence the DOC analysis), and inorganic carbon removal. A portion of each porewater sample was taken and diluted 5 times with Milli-Q water and split into two for DOC measurements using a TOC-L (Shimadzu, Kyoto, Japan) and for the analyses of total Fe, Mn, and S using Inductively coupled plasma atomic emission spectroscopy (ICP-OES) at the University of Delaware Core Laboratory for Soil, Plant, and Water Analysis. Due to lower quantities of porewater in some samples, DOC measurements were prioritized over elemental analyses. The remaining undiluted porewater (if available) was then measured for absorbance at a wavelength of 254 nm using an ultraviolet (UV)-vis spectrophotometer (Agilent Cary 60, Santa Clara, CA). The absorbance was used to calculate the DOM specific UV absorbance ($SUVA_{254}$, L·mg C^{-1}·m^{-1}) based on Eq. 1, which is the ratio of the absorbance at 254 nm (cm^{-1}) to DOC concentration (mg C/L) (Chin et al. 2023):

$$SUVA_{254}\left(L \cdot mgC^{-1} \cdot m^{-1}\right) = \frac{100 \times \text{UV absorbance}_{254nm}(cm^{-1})}{DOC(\text{mg C/L})} \quad (1)$$

Results and discussion

Redox-active species

Depth profiles of O_2, Fe^{2+}, Mn^{2+}, and two potential Fe^{3+}-organic complexes (Fe^{3+}-organics) in sedimentary porewaters were measured for the three cores collected from Toolik and Fog 1 lakes (STL7, STL17, and FL, Figure 2). While each profile was distinct, abundant Fe^{2+} was detected in all three cores and increased in concentration after O_2 became depleted (Figure 2a–c). In addition, we identified two forms of Fe^{3+}-organics (based upon their potentials) in each core both above and below the SWI (Figure 2d–h). While the prevalence and abundance of dissolved Fe^{2+} in these cores indicate the importance of Fe(III) as a TEA, the presence of Fe(III)-organics under anoxic conditions reveals that some fractions were comprised of transient intermediates prior to microbial reduction or stabilized by DOM.

In all three cores, distinctive O_2 peaks were detected above the SWI, yielding O_2 concentrations of 410 µM, 260 µM, and 105 µM at the top of overlying water in STL7, STL17, and FL, respectively. As the cores were collected on different days with highly variable temperatures, the solubility of O_2 in the lake water was calculated (more details in Supporting Information) to check the extent to which the overlying water was saturated with O_2. The solubility of O_2 in lake water on the day STL7, STL17, and FL were collected was 409 µM, 379 µM, and 315 µM, respectively, suggesting the extent of O_2 saturation in overlying water can vary significantly from 30–100 percent depending on temperature, the benthic microbiome, and biogeochemistry. Cores exhibiting lower O_2 saturation coincide with rapid O_2 consumption as a function of depth in the cores. For example, O_2 was only 30 percent saturated at the top of the overlying water and completely depleted above the SWI for FL (Figure 2c), whereas O_2 was 100 percent saturated and penetrated 4 cm below the SWI for STL7 (Figure 2a). The depletion of O_2 at the bottom of overlying lake water in FL is consistent with the bathymetry of the lake where its hypolimnetic volume is quite low. For STL7, O_2 remained relatively constant above the SWI and was moderately depleted at a rate of 12.5 µM mm^{-1} 2 cm below the SWI. This is corroborated by our observations in 2019, where STL9 started with lower O_2 saturation and became depleted above the SWI, whereas STL15 was nearly saturated and penetrated 2 cm below the SWI (Hudson et al. 2022). Spatiotemporal differences in O_2 penetration within Toolik Lake cores between 2019 and the current study may reflect changes in organic carbon loading or hydrodynamic mixing throughout the lake and highlight the dynamic nature of redox "hotspots" (Peiffer et al. 2021; Lacroix et al. 2023; Aeppli et al. 2023).

Reduced TEA species did not appear in the overlying water until O_2 was depleted, i.e., there was almost no overlap between O_2 and either Fe^{2+} or Mn^{2+}. However, once O_2 was depleted, reduced species started to emerge and roughly followed the diagenesis "redox ladder" model (Berner 1980; Luther 2016). Part of this may

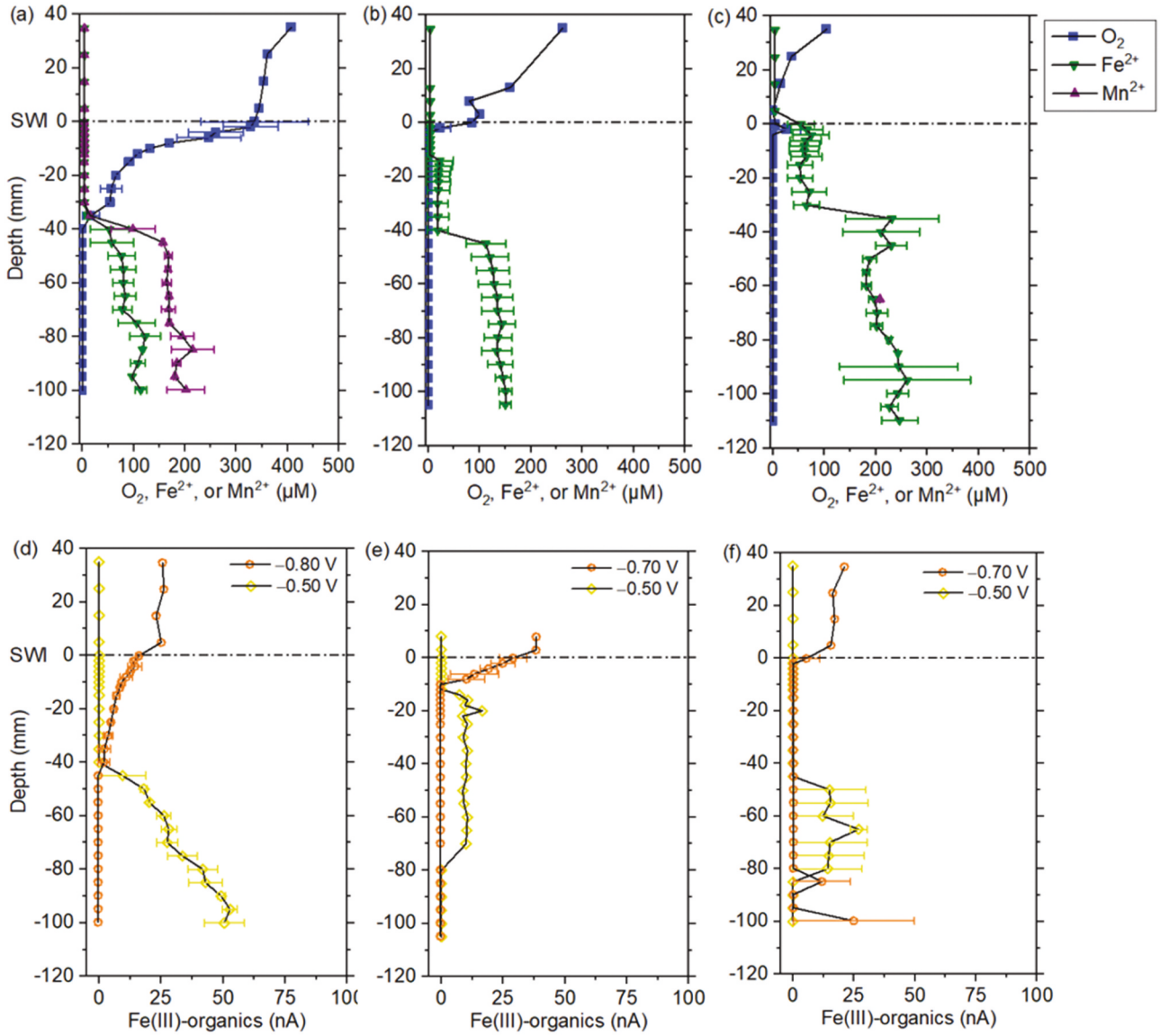

Figure 2. Depth profiles of O_2, Fe^{2+}, and Mn^{2+} concentrations in (a) STL7, (b) STL17, and (c) FL sediment cores and the current response of Fe(III)-organic complexes (Fe(III)-organics) in (d) STL7, (e) STL17, and (f) FL. The results represent an average of measurements at two positions of the same core and error bars are the range from the two measurements.

also be due to the reoxidation of upwardly diffusing Fe^{2+} by O_2, as previously observed by Burdige and Christensen (2022) in the Antarctic Peninsula. In STL7 (Figure 2a), both Fe^{2+} and Mn^{2+} started emerging 4 cm below the SWI due to deep O_2 penetration. The trend of Fe^{2+} and Mn^{2+} concentrations were almost parallel and relatively constant with depth, although Mn^{2+} (~200 μM) was found to be more abundant than Fe^{2+} (~100 μM). As the biological reduction of MnO_2 phases is thermodynamically more favorable than iron oxide phases (Luther et al. 2008; Shufen et al. 2008), a lack of variability in Fe^{2+} and Mn^{2+} trends with depth indicates that biological reduction processes in STL7 favor iron oxides. Consistent with this theory, the depth profiles of total Fe and Mn in STL7 (Figure S2a) showed that the concentrations of Fe and Mn at 6–10 cm depths were ~100 μM and ~400 μM, suggesting that most of Fe existed in its reduced form but only 50 percent Mn was reduced. Despite MnO_2 being a less preferred TEA, the fact that the abundance of Mn^{2+} was higher than that of Fe^{2+} indicates that abiotic Fe^{2+} oxidation by MnO_2 might have happened to certain extents in STL7 (Luther et al. 2008, 2018; Shufen et al. 2008; Luther 2010). In STL17 (Figure 2b), while O_2 was depleted a couple of millimeters below the SWI, Fe^{2+} was not detected abundantly until 4 cm below the SWI. The concentration of Fe^{2+} was < 25 μM until 4 cm depth but increased to ~150 μM in deeper locations. The

comparison between Fe^{2+} and the total Fe (Figure S2b) again showed that most of Fe exists in its reduced form in the porewaters at these depths (below 4 cm). Despite the presence of ~300 μM total Mn, Mn^{2+} was not detected in STL17, which confirms that MnO_2 is not the preferred TEA in Toolik Lake sediments. Although sulfate concentrations were expected to range between 25–50 μM at various depths for both STL7 and STL17 based on the total elemental S concentration (Figure S2), no sulfide signals were detected in either core. The core from FL (Figure 2c) exhibited higher Fe^{2+} concentrations, which were around 75 μM for the first 3 cm and then ranged between 200–300 μM up to 11 cm depth. Similar to STL17, Fe^{2+} was the only reduced species detected in FL, which suggests that Fe(III) is the predominant TEA in all three locations.

Two types of Fe(III)-organics were identified by the CV scan along the depth of all three cores (Figure 2d–h). The first group of Fe(III)-organics, which was reduced at the reduction potential of −0.8 V or −0.7 V (vs. Ag/AgCl), resided in the overlying water and at shallower depths, where O_2 was still present. These ligands (based on their potentials) may correspond to phenolic acids in DOM, which are known to possess large Fe(III) stability constants (e.g., log K > 20) (Buerge and Hug 1999; Sowers et al. 2019; Hudson, George, et al. 2022). The presence of these strong organic ligands in the upper core is unsurprising due to the coprecipitation and adsorption of organic matter to metal oxide surfaces at redox boundaries, which would enhance the mineral dissolution process (Maurice et al. 1995; Kraemer 2004; Chen et al. 2014; Chen and Sparks 2018; Coward, Ohno, and Sparks 2018; Sowers et al. 2019). Due to their relatively low reduction potential, these Fe(III)-organics are very weak oxidants and are unlikely to act as TEAs for iron reducing bacteria. The second group of Fe(III)-organics, which possess a reduction potential of −0.5 V, was present deeper in the core. These weaker ligands, which likely correspond to mono and bidentate carboxylates, might be in higher abundance due to microbial organic matter degradation (Amon et al. 2012; Curti et al. 2021). While less effective than iron oxides, these Fe(III)-organics are stronger oxidants than the first group, suggesting that they could potentially be TEAs deeper in the core. Interestingly, Fe(III)-organics were also found in the 1–4 cm depth of STL17 (Figure 2d), where a lack of both O_2 and free Fe^{2+} was featured (Figure 2b). This suggests that some of the iron oxides undergo dissolution by DOM to form metastable Fe(III) complexes in the porewater prior to microbial reduction to Fe(II) (Kraemer 2004).

Dissolved organic carbon

DOC and $SUVA_{254}$ of sediment porewaters extracted from the three sediment cores (Figure 3) are among the first high spatial resolution DOC measurements of benthic porewater sampled anoxically from Arctic

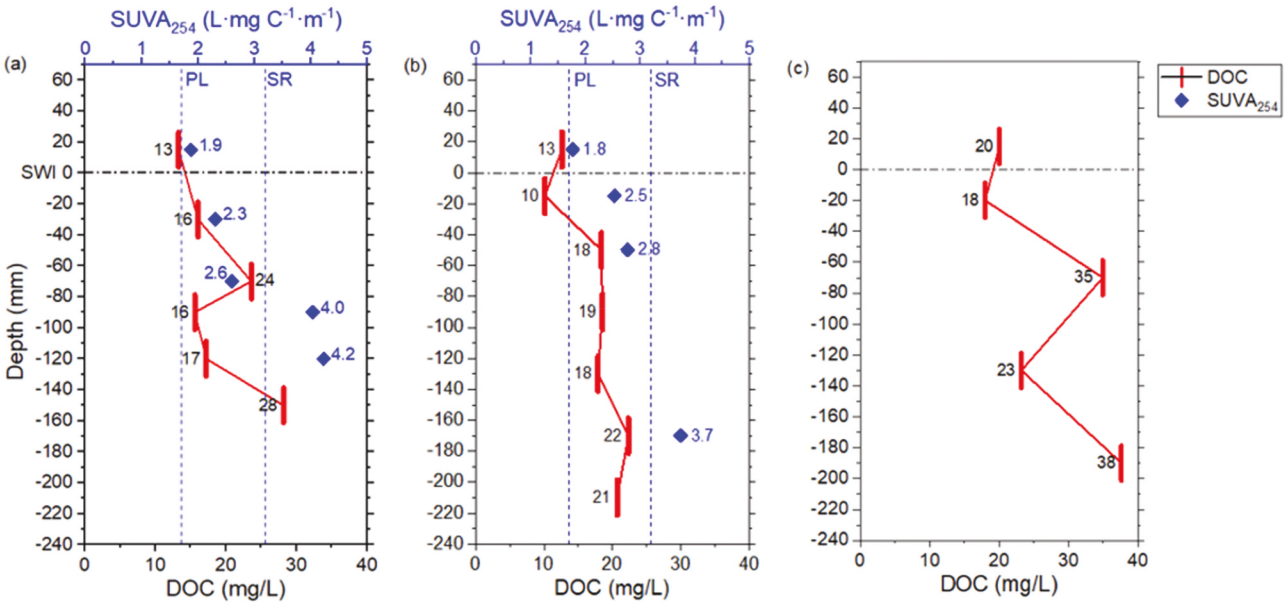

Figure 3. Depth profiles of dissolved organic carbon (DOC) and the specific UV absorbance at 254 nm ($SUVA_{254}$) in porewaters from (a) STL7, (b) STL 17, and (c) FL. Note that only the DOC profile was shown for the FL core due to an insufficient porewater volume. Two vertical reference lines at 1.7 and 3.2 L·mg C^{-1}·m^{-1} are the $SUVA_{254}$ of Pony Lake (PL) fulvic acid and Suwannee River (SR) fulvic acid, respectively.

sediments (Cornwell and Kipphut 1992; Matheus Carnevali et al. 2015). DOC concentrations of overlying water in Toolik Lake and Fog 1 Lake cores were 13 mg/L and 20 mg/L, respectively, higher than previously reported (Cory et al. 2007; Daniels, Kling, and Giblin 2015). We posit that these higher-than-expected DOC values may be partially artifactual due to the upward diffusion of porewater organic matter following core retrieval. DOC concentrations in porewaters from Toolik Lake sediment ranged between 10–28 mg/L (Figure 3a) and showed an increasing trend with the depth of the core in general. This was an expected trend with the accumulation of byproducts from organic matter mineralization (Burdige and Komada 2015) and due to the release of organic matter from solid mineral phases, e.g., iron and manganese oxides, as observed in lower latitude lakes and wetlands (Chin et al. 1998; O'Loughlin and Chin 2004). The DOC concentrations in STL7 (Figure 3a) were mostly in the 16–17 mg/L range, with maximums at depths of 7 cm (24 mg/L) and 15 cm (28 mg/L). The first DOC maximum at around 7 cm closely mirrors the increase in Mn^{2+} and Fe^{2+}, suggesting the release of organics bound to the minerals (Chin et al. 1998; Kraemer 2004; Jang and Brantley 2009). The DOC profile of STL17 was less dynamic than that of STL7 and averaged 18–19 mg/L DOC from 4–15 cm depth with a slight increase to 21–22 mg/L further down the core (Figure 3b). This is also consistent with voltammetric data in Figure 2, which shows steady concentrations of Fe^{2+} down the core, supporting reductive dissolution occurring throughout the core depth (Figure S3, S4). The DOCs (18–38 mg/L) in FL from Fog 1 Lake were overall higher than those from Toolik and showed more variance with depth (Figure 3c). Similar to STL7, the FL DOC concentration profile also revealed two maximums at 7 cm (35 mg/L) and 20 cm (38 mg/L), respectively. For all three cores, the trends of DOC along the depth also appear to correlate with the distribution of Fe(III)-organics (−0.5 V), such as constant DOC at 18–19 mg/L when the Fe(III)-organics signal is around 10 nA in STL17 and spikes in DOC and Fe(III)-organics from 7–9 cm depth of STL7 and at 7 cm depth of FL (Figure S5). This suggests that part of the Fe(III) minerals are released with the above-mentioned reductive dissolution as either Fe(III)-organics or free Fe(III) but immediately formed Fe(III)-organics and stayed meta-stable before being reduced by Fe(III) respiring bacteria.

$SUVA_{254}$ is often used to assess the aromaticity of DOM and the degree of humification. The $SUVA_{254}$ of overlying water of Toolik Lake cores were 1.9 and 1.8, and similar to the microbial endmember Pony Lake Fulvic Acid (1.7 L·mg C^{-1}·m^{-1}) (Weishaar et al. 2003), suggesting that pelagic primary and heterotrophic activity (Cawley et al. 2013) might be the main precursor of DOC in overlying waters during the Arctic summer. Additionally, low values near the SWI suggest preferential adsorption of aromatic DOM fractions to metal-oxide surfaces such as iron oxides due to their circumneutral zero point of charge, thereby leaving more aromatic-depleted organic matter in pore fluids (Meier et al. 1999; Meier, Chin, and Maurice 2004). This process seems likely when comparing Fe(III)-organics voltammetric data to SUVA data (Figure S5). The increased strong-ligand signal at the top of the core suggests enrichment of stronger ligands associated with metal-oxides, depleting SUVA values. The $SUVA_{254}$ of porewaters increased with the depth, surpassing values reported for the terrestrial DOM reference, Suwannee River fulvic acid, suggesting the release of more aromatic DOC as bio-mediated reductive dissolution of iron oxide occurs deeper in the core coupled with humification processes (Chin et al. 1998).

The $SUVA_{254}$ of porewaters at shallower depths (above 8 cm) ranged from 2.3 to 2.8, which lies between the two DOM geochemical endmembers Pony Lake fulvic acid (1.7 L·mg C^{-1}·m^{-1}) and Suwannee River fulvic acid (3.2 L·mg C^{-1}·m^{-1}, Weishaar et al. 2003; Chin et al. 2023). In a couple of cases $SUVA_{254}$ increased to > 4.0 L·mg C^{-1}·m^{-1} at around 12 cm depth of STL7. These high values could be interference from soluble iron (Figure S3, S4), which can absorb light at the same wavelength and is also high in concentration at this depth (Weishaar et al. 2003). Due to the small volumes of porewater extracted from FL, we were not able to obtain $SUVA_{254}$ values for this site.

Temporal variation of Toolik Lake

The distribution of redox-active species in Toolik Lake sedimentary porewaters was measured in 2019 and reported by Hudson et al. (2022). We attempted to sample as close to the 2019 locations to minimize spatial variability and enable a temporal comparison. Fe^{2+} was ubiquitously found in all cores collected from the southwest side of Toolik Lake, whereas Mn^{2+} was only found in selected cores (STL9 and STL10 in 2019, and STL7 in 2022). The prevalence of Fe^{2+} and the unpredictable distribution of Mn^{2+} in Toolik cores remained consistent from 2019 to the present study. The highest concentration of Fe^{2+} in the Toolik porewater from this study was 150 μM, which was lower than that in the 2019 study (up to 300 μM in STL9 and STL15). Further, Fe^{2+} and Mn^{2+} concentrations in STL7 from this study were very similar to those measured in STL10 from 2019. This suggests some temporal consistency of redox-

active species in Toolik Lake benthic porewaters, but specific concentrations of Fe^{2+} and Mn^{2+} can vary over relatively fine (10′s of meters) area resolution (Cornwell and Kipphut 1992).

The results from our two studies were also consistent in that O_2 diffusion downcore (STL15 in 2019, and STL7 in 2022) and parallel trends for Fe^{2+} and Mn^{2+} along the depth (STL10 in 2019, STL7 in 2022) were observed in the studied cores. Similar O_2 penetration and parallel Fe^{2+} and Mn^{2+} distributions were also found in a core (ETL10 in 2019) collected near the East side of the Toolik Lake (Hudson et al. 2022). Among all the cores analyzed (from 2019 and 2022), STL7 from this study exhibited the deepest O_2 penetration into the sediments (4 cm) and was even 2 cm deeper than the STL15 core from the 2019 study. Thus, O_2 distribution varied greatly both spatially and temporally over the two sampling events. This demonstrates that the biogeochemical processes at the SWI are complex, which when coupled with hydrodynamics within the water column will likely result in patchy as opposed to uniform patterns for overall element cycling in Arctic lakes (MacIntyre et al. 2009; MacIntyre, Cortés, and Sadro 2018). The overall spatial variations observed across different locations and the shifting distribution of redox species in each core with depth at Toolik Lake are consistent with sediment porewaters observed elsewhere (Hakala et al. 2009). Further, this lake, characterized by multiple basin kettles, naturally exhibits more heterogeneity compared to other settings.

Summary and environmental implications

This study is the first to report coupled high spatial measurements of redox-active species and DOC from multiple sites in Arctic lacustrine porewaters, while past studies have only measured one or the other (Cornwell and Kipphut 1992; Matheus Carnevali et al. 2015). The study reveals processes that tightly couple TEAs and DOM in sedimentary porewaters, which may play a critical role in shaping the Arctic benthic microbiome. The comparison between the cores collected from Fog 1 Lake (FL) and Toolik Lake (STL7 and STL17) reveals a higher accumulation of Fe^{2+} and DOM in Fog 1 than Toolik, which could be due to the differences in hydrology, lake productivity, and water chemistries (e.g., alkalinity) (Giblin and Kling 2016). For all three cores, abundant Fe^{2+} was detected at or below 4 cm of the SWI and is inversely related to dissolved O_2. While the distribution of redox-active species for all our sediment cores roughly followed the diagenetic "redox ladder" model (Berner 1980; Luther 2016), some Fe(III) remained (meta)stable under reducing conditions due to the formation of Fe(III)-DOM complexes (Luther et al. 1992; Luther, Shellenbarger, and Brendel 1996; Hakala et al. 2009).

The speciation and concentration of redox-active species in the benthic zone and immediate overlying water varied both spatially and temporally. Voltammetric data obtained from Toolik Lake (STL7 and STL17) in 2022 differed from the data obtained in adjacent sites (STL9 and STL15) in 2019. This highlights the "patchy" spatiotemporal nature of TEAs in lacustrine sediments. Porewater DOCs in Toolik sediment cores were also lower than values reported for lower latitude lakes (Chin et al. 1998; O'Loughlin and Chin 2004; Hakala et al. 2009) and are likely due to the highly oligotrophic nature of these water bodies. Spikes in DOC and $SUVA_{254}$, however, did roughly occur at the same depth as increases in Fe^{2+}, suggesting the release of more aromatic DOM through the reductive dissolution of iron oxides.

Destabilization of permafrost, the development of thermokarsts, and prolonged ice-free seasons in the Arctic would result in a positive feedback loop for carbon, releasing it into the air through heterotrophic activity (Walter Anthony et al. 2016; Turetsky et al. 2020; Miner et al. 2022). The degree of this feedback loop is driven by the type and availability of organic carbon sources and TEAs in the microbiome. Our research represents one of the pioneering efforts to assess the types and spatiotemporal distributions of TEAs and DOM in Arctic sedimentary porewaters. Our findings lay the groundwork for further investigations into the nature of microbial communities in these environments and their roles in carbon cycling, including potential negative feedback mechanisms, such as carbon preservation through DOM-TEA complexes.

Acknowledgments

This research is funded by NSF grant CBET 1804611. The authors gratefully acknowledge logistical support provided by staff at Toolik Field Station (University of Alaska Fairbanks) and field assistance provided by Alexander B. Michaud and David Emerson (Bigelow Laboratory for Ocean Science).

Disclosure statement

No potential conflict of interest was reported by the author(s).

Funding

This work was supported by the National Science Foundation [CBET 1804611].

ORCID

Jeffrey M. Hudson http://orcid.org/0000-0002-6630-6331
Yu-Ping Chin http://orcid.org/0000-0003-1427-9156

References

Aeppli, M., A. Thompson, C. Dewey, and S. Fendorf. 2022. Redox properties of solid phase electron acceptors affect anaerobic microbial respiration under oxygen-limited conditions in floodplain soils. *Environmental Science and Technology* 56, no. 23:17462–70. doi:10.1021/acs.est.2c05797.

Aeppli, M., S. Vranic, R. Kaegi, R. Kretzschmar, A. R. Brown, A. Voegelin, T. B. Hofstetter, and M. Sander. 2019. Decreases in iron oxide reducibility during microbial reductive dissolution and transformation of ferrihydrite. *Environmental Science and Technology* 53, no. 15:8736–46. doi:10.1021/acs.est.9b01299.

Amon, R. M. W., A. J. Rinehart, S. Duan, P. Louchouarn, A. Prokushkin, G. Guggenberger, D. Bauch, C. Stedmon, P. A. Raymond, and R. M. Holmes. 2012. Dissolved organic matter sources in large Arctic rivers. *Geochimica et Cosmochimica Acta* 94:217–37. doi:10.1016/j.gca.2012.07.015.

Angle, J. C., T. H. Morin, L. M. Solden, A. B. Narrowe, G. J. Smith, M. A. Borton, C. Rey-Sanchez, R. A. Daly, G. Mirfenderesgi, and D. W. Hoyt. 2017. Methanogenesis in oxygenated soils is a substantial fraction of wetland methane emissions. *Nature Communications* 8, no. 1:1567. doi:10.1038/s41467-017-01753-4.

Barker, A. J., T. D. Sullivan, W. Brad Baxter, R. A. Barbato, S. Gallaher, G. E. Patton, J. P. Smith, and T. A. Douglas. 2023. Iron oxidation–reduction processes in warming permafrost soils and surface waters expose a seasonally rusting Arctic watershed. *ACS Earth and Space Chemistry* 7, no. 8:1479–95. doi:10.1021/acsearthspacechem.2c00367.

Berner, R. A. 1980. *Early diagenesis: A theoretical approach*. Princeton, NJ: Princeton University Press.

Buerge, I. J., and S. J. Hug. 1999. Influence of mineral surfaces on Chromium(VI) reduction by Iron(II). *Environmental Science and Technology* 33, no. 23:4285–91. doi:10.1021/es981297s.

Burdige, D. J., M. J. Alperin, J. Homstead, and C. S. Martens. 1992. The role of benthic fluxes of dissolved organic carbon in oceanic and sedimentary carbon cycling. *Geophysical Research Letters* 19, no. 18:1851–4. doi:10.1029/92GL02159.

Burdige, D. J., and J. P. Christensen. 2022. Iron biogeochemistry in sediments on the western continental shelf of the Antarctic Peninsula. *Geochimica et Cosmochimica Acta* 326:288–312. doi:10.1016/j.gca.2022.03.013.

Burdige, D. J., and T. Komada. 2015. Sediment pore waters. In *Biogeochemistry of marine dissolved organic matter*, ed. D. A. Hansell and C. A. Carlson, 533–577. 2nd ed. Cambridge, MA: Elsevier.

Cawley, K. M., D. M. McKnight, P. Miller, R. Cory, R. L. Fimmen, J. Guerard, M. Dieser, C. Jaros, Y.-P. Chin, and C. Foreman. 2013. Characterization of fulvic acid fractions of dissolved organic matter during ice-out in a hyper-eutrophic, coastal pond in Antarctica. *Environmental Research Letters* 8, no. 4:045015. doi:10.1088/1748-9326/8/4/045015.

Chan, C. S., D. Emerson, and G. W. Luther. 2016. The role of microaerophilic Fe-oxidizing micro-organisms in producing banded iron formations. *Geobiology* 14, no. 5:509–28. doi:10.1111/gbi.12192.

Chen, C., J. J. Dynes, J. Wang, and D. L. Sparks. 2014. Properties of Fe-organic matter associations via coprecipitation versus adsorption. *Environmental Science and Technology* 48, no. 23:13751–9. doi:10.1021/es503669u.

Chin, Y.-P., D. M. McKnight, J. D'Andrilli, N. Brooks, K. Cawley, J. Guerard, E. M. Perdue, et al. 2023. Identification of next-generation International Humic Substances Society reference materials for advancing the understanding of the role of natural organic matter in the Anthropocene. *Aquatic Sciences* 85, no. 1:32. doi:10.1007/s00027-022-00923-x.

Chin, Y.-P., S. J. Traina, C. R. Swank, and D. Backhus. 1998. Abundance and properties of dissolved organic matter in pore waters of a freshwater wetland. *Limnology and Oceanography* 43, no. 6:1287–96. doi:10.4319/lo.1998.43.6.1287.

Chunmei, C., and D. L. Sparks. 2018. Fe(II)-induced mineral transformation of ferrihydrite–organic matter adsorption and co-precipitation complexes in the absence and presence of As(III). *ACS Earth and Space Chemistry* 2, no. 11:1095–101. doi:10.1021/acsearthspacechem.8b00041.

Cornwell, J. C., and G. W. Kipphut. 1992. Biogeochemistry of manganese- and iron-rich sediments in Toolik Lake, Alaska. *Hydrobiologia* 240, no. 1–3:45–59.

Cory, R. M., D. M. McKnight, Y.-P. Chin, P. Miller, and C. L. Jaros. 2007. Chemical characteristics of fulvic acids from arctic surface waters: Microbial contributions and photochemical transformations. *Journal of Geophysical Research: Biogeosciences* 112, no. G4. doi:10.1029/2006JG000343.

Coward, E. K., T. Ohno, and D. L. Sparks. 2018. Direct evidence for temporal molecular fractionation of dissolved organic matter at the iron oxyhydroxide interface. *Environmental Science and Technology* 53, no. 2:642–50. doi:10.1021/acs.est.8b04687.

Curti, L., O. W. Moore, P. Babakhani, K.-Q. Xiao, C. Woulds, A. W. Bray, B. J. Fisher, M. Kazemian, B. Kaulich, and C. L. Peacock. 2021. Carboxyl-richness controls organic carbon preservation during coprecipitation with iron (oxyhydr)oxides in the natural environment. *Communications Earth & Environment* 2, no. 1:229. doi:10.1038/s43247-021-00301-9.

Dalcin Martins, P., D. W. Hoyt, S. Bansal, C. T. Mills, M. Tfaily, B. A. Tangen, R. G. Finocchiaro, et al. 2017. Abundant carbon substrates drive extremely high sulfate reduction rates and methane fluxes in Prairie Pothole Wetlands. *Global Change Biology* 23, no. 8:3107–20. doi:10.1111/gcb.13633.

Daniels, W. C., G. W. Kling, and A. E. Giblin. 2015. Benthic community metabolism in deep and shallow Arctic lakes during 13 years of whole–lake fertilization. *Limnology and Oceanography* 60, no. 5:1604–18. doi:10.1002/lno.10120.

Druschel, G. K., R. S. David Emerson, G. W. Luther, and G. W. Luther. 2008. Low-oxygen and chemical kinetic constraints on the geochemical niche of neutrophilic iron(II) oxidizing microorganisms. *Geochimica et Cosmochimica Acta* 72, no. 14:3358–70. doi:10.1016/j.gca.2008.04.035.

Giblin, A. E., and G. W. Kling. 2016. Water chemistry data for various lakes near Toolik Research Station, ArcticLTER. Summer 2000 to 2009. ver 4. *Environmental Data Initiative*. https://portal.edirepository.org/nis/mapbrowse?packageid=knb-lter-arc.10090.4

Hakala, J. A., R. L. Fimmen, Y.-P. Chin, S. G. Agrawal, and C. P. Ward. 2009. Assessment of the geochemical reactivity of Fe-DOM complexes in wetland sediment pore waters using a nitroaromatic probe compound. *Geochimica et Cosmochimica Acta* 73, no. 5:1382–93. doi:10.1016/j.gca.2008.12.001.

Hudson, J., M. George, W. Luther III, and Y.-P. Chin. 2022. Influence of organic ligands on the redox properties of Fe (II) as determined by mediated electrochemical oxidation. *Environmental Science and Technology* 56, no. 12:9123–32. doi:10.1021/acs.est.2c01782.

Hudson, J. M., A. B. Michaud, D. Emerson, and Y.-P. Chin. 2022. Spatial distribution and biogeochemistry of redox active species in arctic sedimentary porewaters and seep. *Environmental Science: Processes & Impacts* 24, no. 3:426–38. doi:10.1039/D1EM00505G.

Jang, J.-H., and S. L. Brantley. 2009. Investigation of Wüstite (FeO) dissolution: Implications for reductive dissolution of ferric oxides. *Environmental Science and Technology* 43, no. 4:1086–90. doi:10.1021/es8010139.

Kaiser, K., and G. Guggenberger. 2000. The role of DOM sorption to mineral surfaces in the preservation of organic matter in soil. *Organic Geochemistry* 31, no. 7–8:711–25. doi:10.1016/S0146-6380(00)00046-2.

Kraemer, S. M. 2004. Iron oxide dissolution and solubility in the presence of siderophores. *Aquatic Sciences - Research Across Boundaries* 66, no. 1:3–18. doi:10.1007/s00027-003-0690-5.

Krepski, S. T., D. Emerson, P. L. Hredzak-Showalter, G. W. Luther, and C. S. Chan. 2013. Morphology of biogenic iron oxides records microbial physiology and environmental conditions: Toward interpreting iron microfossils. *Geobiology* 11, no. 5:457–71. doi:10.1111/gbi.12043.

Lacroix, E. M., M. Aeppli, K. Boye, E. Brodie, S. Fendorf, M. Keiluweit, H. R. Naughton, V. Noël, and D. Sihi. 2023. Consider the anoxic microsite: Acknowledging and appreciating spatiotemporal redox heterogeneity in soils and sediments. *ACS Earth and Space Chemistry* 7, no. 9:1592–609. doi:10.1021/acsearthspacechem.3c00032.

Lalonde, K., A. Mucci, A. Ouellet, and Y. Gélinas. 2012. Preservation of organic matter in sediments promoted by iron. *Nature* 483, no. 7388:198–200. doi:10.1038/nature10855.

Levine, M. A., and S. C. Whalen. 2001. Nutrient limitation of phytoplankton production in Alaskan Arctic foothill lakes. *Hydrobiologia* 455, no. 1/3:189–201. doi:10.1023/A:1011954221491.

Liang, W., X. Chen, C. Zhao, L. Ling, and H. Ding. 2023. Seasonal changes of dissolved organic matter chemistry and its linkage with greenhouse gas emissions in saltmarsh surface water and porewater interactions. *Water Research* 245:120582. doi:10.1016/j.watres.2023.120582.

Luther, G. W., III. 2010. The role of one- and two-electron transfer reactions in forming thermodynamically unstable intermediates as barriers in multi-electron redox reactions. *Aquatic Geochemistry* 16, no. 3:395–420. doi:10.1007/s10498-009-9082-3.

Luther, G. W., III. 2016. *Inorganic chemistry for geochemistry and environmental sciences: Fundamentals and applications*. Chichester: John Wiley & Sons.

Luther, G. W., III, B. T. Glazer, M. Shufen, R. E. Trouwborst, T. S. Moore, E. Metzger, C. Kraiya, et al. 2008. Use of voltammetric solid-state (micro)electrodes for studying biogeochemical processes: Laboratory measurements to real time measurements with an *in situ* electrochemical analyzer (ISEA). *Marine Chemistry* 108, no. 3–4:221–35. doi:10.1016/j.marchem.2007.03.002.

Luther, G. W., III, J. E. Kostka, T. M. Church, B. Sulzberger, and W. Stumm. 1992. Seasonal iron cycling in the salt-marsh sedimentary environment: the importance of ligand complexes with Fe(II) and Fe(III) in the dissolution of Fe (III) minerals and pyrite, respectively. *Marine Chemistry* 40, no. 1–2:81–103. doi:10.1016/0304-4203(92)90049-G.

Luther, G. W., III, P. A. Shellenbarger, and J. B. Paul. 1996. Dissolved organic Fe(III) and Fe(II) complexes in salt marsh porewaters. *Geochimica et Cosmochimica Acta* 60, no. 6:951–60. doi:10.1016/0016-7037(95)00444-0.

Luther, G. W., III, A. Thibault De Chanvalon, V. E. Oldham, E. R. Estes, B. M. Tebo, and A. S. Madison. 2018. Reduction of manganese oxides: Thermodynamic, kinetic and mechanistic considerations for one- versus two-electron transfer steps. *Aquatic Geochemistry* 24, no. 4:257–77. doi:10.1007/s10498-018-9342-1.

MacIntyre, S., A. Cortés, and S. Sadro. 2018. Sediment respiration drives circulation and production of CO_2 in ice-covered Alaskan arctic lakes. *Limnology and Oceanography Letters* 3, no. 3:302–10. doi:10.1002/lol2.10083.

MacIntyre, S., J. P. Fram, P. J. Kushner, N. D. Bettez, W. J. O'Brien, J. E. Hobbie, and G. W. Kling. 2009. Climate-related variations in mixing dynamics in an Alaskan arctic lake. *Limnology and Oceanography* 54, no. 6part2:2401–17. doi:10.4319/lo.2009.54.6_part_2.2401.

Matheus Carnevali, P. B., M. Rohrssen, M. R. Williams, A. B. Michaud, H. Adams, D. Berisford, G. D. Love, J. C. Priscu, O. Rassuchine, and K. P. Hand. 2015. Methane sources in arctic thermokarst lake sediments on the North Slope of Alaska. *Geobiology* 13, no. 2:181–97. doi:10.1111/gbi.12124.

Maurice, P. A., M. F. Hochella, G. A. Parks, G. Sposito, and U. Schwertmann. 1995. Evolution of hematite surface microtopography upon dissolution by simple organic acids. *Clays and Clay Minerals* 43, no. 1:29–38. doi:10.1346/CCMN.1995.0430104.

McAdams, B. C., R. M. Adams, W. A. Arnold, and Y.-P. Chin. 2016. Novel insights into the distribution of reduced sulfur species in prairie pothole wetland porewaters provided by bismuth film electrodes. *Environmental Science & Technology Letters* 3, no. 3:104–9. doi:10.1021/acs.estlett.6b00020.

McAdams, B. C., W. A. Arnold, M. J. Wilkins, and Y. P. Chin. 2021. Ice cover influences redox dynamics in prairie pothole wetland sediments. *Journal of Geophysical Research:*

Biogeosciences 126, no. 10:e2021JG006318. doi:10.1029/2021JG006318.

Meier, M., Y.-P. Chin, and P. Maurice. 2004. Variations in the composition and adsorption behavior of dissolved organic matter at a small, forested watershed. *Biogeochemistry* 67, no. 1:39–56. doi:10.1023/B:BIOG.0000015278.23470.f7.

Meier, M., K. Namjesnik-Dejanovic, P. A. Maurice, Y.-P. Chin, and G. R. Aiken. 1999. Fractionation of aquatic natural organic matter upon sorption to goethite and kaolinite. *Chemical Geology* 157, no. 3–4:275–84. doi:10.1016/S0009-2541(99)00006-6.

Meret, A., G. Schladow, J. S. Lezama Pacheco, and S. Fendorf. 2023. Iron reduction in profundal sediments of Ultraoligotrophic Lake Tahoe under oxygen-limited conditions. *Environmental Science and Technology* 57, no. 3:1529–37. doi:10.1021/acs.est.2c05714.

Michael, A., M. Sander, and R. P. Schwarzenbach. 2010. Novel electrochemical approach to assess the redox properties of humic substances. *Environmental Science and Technology* 44, no. 1:87–93. doi:10.1021/es902627p.

Miner, K. R., M. R. Turetsky, E. Malina, A. Bartsch, A. D. M. Johanna Tamminen, A. Fix, C. Sweeney, C. D. Elder, and C. E. Miller. 2022. Permafrost carbon emissions in a changing Arctic. *Nature Reviews Earth & Environment* 3, no. 1:55–67. doi:10.1038/s43017-021-00230-3.

O'Loughlin, E. J., and Y.-P. Chin. 2004. Quantification and characterization of dissolved organic carbon and iron in sedimentary porewater from Green Bay, WI, USA. *Biogeochemistry* 71, no. 3:371–86. doi:10.1007/s10533-004-0373-x.

Peiffer, S., A. Kappler, S. B. Haderlein, C. Schmidt, J. M. Byrne, S. Kleindienst, C. Vogt, et al. 2021. A biogeochemical–hydrological framework for the role of redox-active compounds in aquatic systems. *Nature Geoscience* 14, no. 5:264–72. doi:10.1038/s41561-021-00742-z.

Schuur, E. A. G., B. W. Abbott, R. Commane, J. Ernakovich, E. Euskirchen, G. Hugelius, G. Grosse, et al. 2022. Permafrost and climate change: Carbon cycle feedbacks from the warming Arctic. *Annual Review of Environment and Resources* 47, no. 1:343–71. doi:10.1146/annurev-environ-012220-011847.

Shufen, M., G. W. Luther, J. Keller, A. Madison, E. Metzger, D. Emerson, and J. Megonigal. 2008. Solid-state Au/Hg microelectrode for the investigation of Fe and Mn cycling in a freshwater wetland: Implications for methane production. *Electroanalysis* 20, no. 3:233–9. doi:10.1002/elan.200704048.

Sowers, T. D., K. L. Holden, E. K. Coward, and D. L. Sparks. 2019. Dissolved organic matter sorption and molecular fractionation by naturally occurring bacteriogenic iron (oxyhydr)oxides. *Environmental Science and Technology* 53, no. 8:4295–304. doi:10.1021/acs.est.9b00540.

Trusiak, A., L. A. Treibergs, G. W. Kling, and R. M. Cory. 2018. The role of iron and reactive oxygen species in the production of CO_2 in arctic soil waters. *Geochimica et Cosmochimica Acta* 224:80–95. doi:10.1016/j.gca.2017.12.022.

Turetsky, M. R., B. W. Abbott, M. C. Jones, K. Walter Anthony, D. Olefeldt, E. A. G. Schuur, G. Grosse, et al. 2020. Carbon release through abrupt permafrost thaw. *Nature Geoscience* 13, no. 2:138–43. doi:10.1038/s41561-019-0526-0.

Uffe, T., B. Thamdrup, D. A. Stahl, and D. E. Canfield. 2004. Pathways of organic carbon oxidation in a deep lacustrine sediment, Lake Michigan. *Limnology and Oceanography* 49, no. 6:2046–57. doi:10.4319/lo.2004.49.6.2046.

Walpen, N., G. J. Getzinger, M. H. Schroth, and M. Sander. 2018. Electron-donating phenolic and electron-accepting quinone moieties in peat dissolved organic matter: Quantities and redox transformations in the context of peat biogeochemistry. *Environmental Science and Technology* 52, no. 9:5236–45. doi:10.1021/acs.est.8b00594.

Walter Anthony, K., R. Daanen, P. Anthony, T. Schneider Von Deimling, C.-L. Ping, J. P. Chanton, and G. Grosse. 2016. Methane emissions proportional to permafrost carbon thawed in Arctic lakes since the 1950s. *Nature Geoscience* 9, no. 9:679–82. doi:10.1038/ngeo2795.

Weishaar, J. L., G. R. Aiken, B. A. Bergamaschi, M. S. Fram, R. Fujii, and K. Mopper. 2003. Evaluation of specific ultraviolet absorbance as an indicator of the chemical composition and reactivity of dissolved organic carbon. *Environmental Science and Technology* 37, no. 20:4702–8. doi:10.1021/es030360x.

Wenk, J., M. Aeschbacher, E. Salhi, S. Canonica, U. von Gunten, and M. Sander. 2013. Chemical oxidation of dissolved organic matter by chlorine dioxide, chlorine, and ozone: Effects on its optical and antioxidant properties. *Environmental Science and Technology* 47, no. 19:11147–56. doi:10.1021/es402516b.